Max-Born-Preis

The Structure of Hadronic Physics

John Dainton

The phenomenology of hadronic interactions at high energy, which developed in the 1960s, is briefly explained. Following the introduction of Quantum Chromodynamics (QCD) and its success in elucidating the nature of nucleon structure in the 1970s, experimental results, both new and not so new, are described which, when taken together, provide insight into the structure of hadrons and of the chromodynamic mechanisms responsible for their interactions.

Nearly every advance in physics can be attributed in some way or another to an understanding of the structure of the phenomenon on which it is based. Measurements of structure come from scattering experiments in which the results depend on the nature both of the quanta involved and of their interaction, sometimes in an inseparable way. They rely on the principles of quantum mechanics embodied in Heisenberg's Uncertainty Principle [1, 2, 3]

$$\Delta T \cdot \Delta E \gtrsim \hbar \ , \quad \Delta \boldsymbol{r} \cdot \Delta \boldsymbol{p} \gtrsim \hbar \ . \qquad (1)$$

Particle Physics is no exception. It is driven by a wish to get to the simplest explanation for the reason why matter is the way it is. Thus it is concerned with the scattering of particles at the highest possible energy in which the shortest distances and the shortest time intervals can be resolved.

The results of scattering experiments come in the form of measurements of the spectroscopy of excitation, such as in figure 1a, or in measurements of scattering angular distributions, such as in figure 1b, and the extraction from them of form factors and structure functions. The final state in each case can be either two individual particles or two groups of particles which move together.

In this presentation I wish to explain the present state of our understanding of hadronic physics. The mass of the universe is attributable in very large part to hadrons, that is to neutrons and protons and to their excitations. The physics of hadrons is therefore central to our understanding of the universe. Nearly everything which we know about hadrons is from scattering experiments, following the time–honoured experimental principles outlined above.

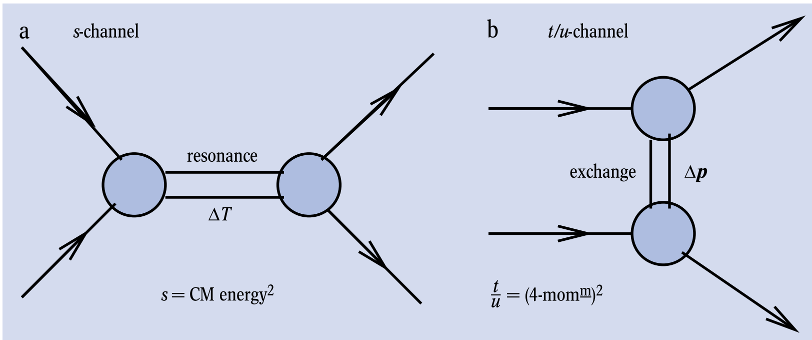

Fig. 1:
▶ a) Particle spectroscopy: the formation and subsequent decay of a resonance, or excited state of two particles interacting with each other with an interaction energy corresponding to the invariant mass $M = \sqrt{s}$ of the resonance; the resonance is excited provided the interaction energy differs from the resonance mass by no more than $\Delta E \sim \Delta M$ which is related to the lifetime (ΔT) of the excited state according to the Heisenberg Uncertainty principle (equation 1). The dynamics of the interaction is said to be dominated by a resonance or exchange "in the s–channel".
▶ b) The scattering of two particles with momentum transfer $\Delta \boldsymbol{p}$ in which structure of spatial dimension $\Delta \boldsymbol{r}$ is visible due to any or all of the incident particles and their interaction; $\Delta \boldsymbol{p}$ and $\Delta \boldsymbol{r}$ are related according to the Heisenberg Uncertainty principle equation 1 in the text.

In the Beginning

The first steps in understanding the structure of hadronic physics came from measurements of the dependence on interaction energy and momentum transfer of hadron scattering. Hadronic "resonances" were observed and their properties and quantum numbers were determined (figure 1a). Thereby a spectroscopy of hadrons emerges [4] in terms of that of quarks of different "flavour" up u, down d, and more [5]. Three quarks, uud, constitute the proton. When in 1964 this spectroscopy was first noticed, there was a conspicuous lack of experimental evidence for the existence of such quarks as identifiable quanta.

At much higher energy the dependences of these scattering processes on momentum transfer, or scattering angle, are found to have features reminiscent of diffraction in optics, or diffraction in X–ray and neutron scattering by crystalline material. For example in proton–proton elastic scattering $pp \to pp$, figure 2a, structure in the interaction is self–evident if one thinks in terms of diffraction [6].

Such scattering favours small scattering angles, that is small $|t|$ – t is the 4–momentum transfer squared in

Prof. John Dainton, Oliver Lodge Laboratory, Department of Physics, The University of Liverpool, UK and DESY, Hamburg, Germany – Plenary talk given at the 63. Physikertagung Heidelberg on the occasion of the conferment of the Max Born Prize

Physikalische Blätter
55 (1999) Nr. 7/8
0031-9279/99/0707-75
$17.50+50/0

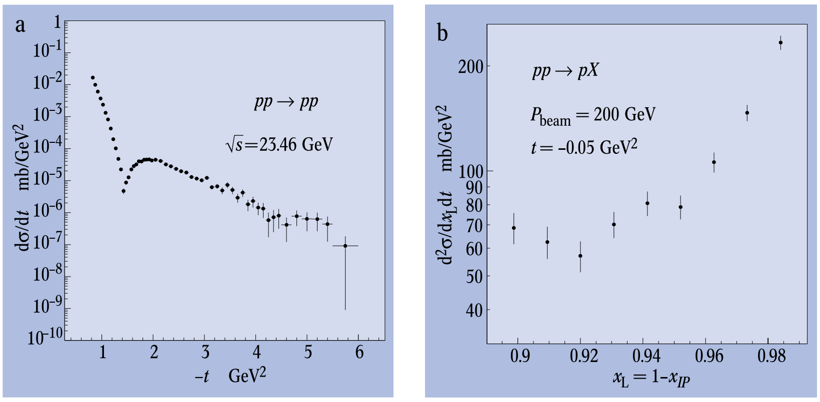

Fig. 2:
▶ a) The differential cross section $d\sigma/dt$ for the process $\bar{p}p \to \bar{p}p$ [6]; t is the 4-momentum transfer squared in the interaction; a clear "diffraction-like" structure is visible. Not shown are measurements for $t > -0.6\,\mathrm{GeV}^2$ for which the peripheral dependence of $d\sigma/dt$ continues upwards to the kinematic limit at $t \to 0\,\mathrm{GeV}^2$.
▶ b) The differential cross section $d\sigma/dt\,dx_L$ for the inclusive production $pp \to pX$ at $t = -0.05\,\mathrm{GeV}^2$ as a function of longitudinal momentum x_L expressed as a fraction of the incident proton momentum [7]; when x_L is large ($x_P = 1 - x_L$ small) the cross section $\sim 1/x_P$.

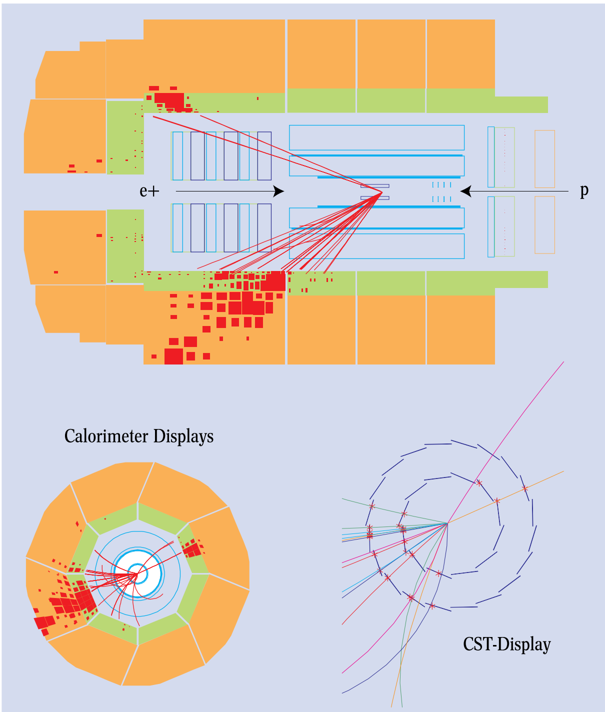

Fig. 3:
A deeply inelastic electron–proton interaction in the H1 experiment at HERA; a positron e^+ with energy 27.5 GeV from the left collides head–on with a proton p with energy 820 GeV from the right (upper calorimeter display); the positron is "back-scattered" due to the high 4–momentum transfer squared Q^2, and is reconstructed as a track pointing to a cluster of energy in the calorimeter; the proton fragments in the form of a "jet" of many tracks and associated cluster corresponding to the direction of the quark in the proton which is resolved and struck by the positron (both calorimeter displays); fragments from the remnant of the proton stay undetected in the direction of the proton beam; both a "side view" and the incident proton's "eye view" are shown; the CST–display shows the hits from the traversal of charged particles, both the scattered positron and those in the quark jet, and the result of reconstructing these hits into trajectories of the charged particles in the axial magnetic field of the H1 experiment; the positron is seen to "balance" the jet of hadrons in direction reflecting the conservation of momentum perpendicular to the direction of the electron and proton beams.

the interaction (figure 2a). The interactions are said to be peripheral[1]. Furthermore, for inelastic processes like $pp \to Xp$, interactions are favoured in which there is very little loss of momentum by the incident proton (figure 2b) [7]. Here X is a cluster of hadrons distinguished in the final state Xp by the fact that it includes more than one particle moving together and balancing the momentum of the proton.

Remarkable insight into the structure of hadronic physics is obtained from these observations. The peripheral nature of the interactions, namely that the momentum transfer $\Delta\boldsymbol{p}$ ($\sim(-t)^{1/2}$) is predominantly less than 1 GeV, means that the spatial extent of the whole scattering process is typically greater than 0.2 fm (equation 1)[2]. The bulk of the interaction cross section can therefore not depend on the single individual interactions of the components of the hadrons (nowadays known to be quarks), but on some sort of collective phenomenon of them. With this in mind a simple and elegant idea, first proposed by Yukawa many years before such observations were first made [8], can be used as a basis of an understanding of these interactions. Yukawa proposed that the action between two interacting particles could be attributed to the exchange of another particle. In terms of figure 1b, when two hadrons interact the momentum $\Delta\boldsymbol{p}$ is transferred by the exchange of a third hadron.

Yukawa's original and beautiful idea is nowadays encapsulated in a theory of scattering amplitudes developed by Regge [9]. Application of a phenomenology based on this approach is found to be very successful. This success is all the more remarkable because the phenomenology does not depend on any detailed knowledge of the structure of the individual hadrons themselves.

To go further and establish a theory of these interactions requires experiments which can resolve the structure of hadrons and their interactions. In such measurements the size $\Delta\boldsymbol{p}$ of the momentum transfer must correspond to a spatial resolution $\sim\hbar/\Delta p$ (equation 1) which is much smaller than hadronic dimension ($\sim$1 fm).

The Structure of the Proton

In the pursuit of hadronic structure it is natural to try to use point–like particles to probe in scattering experiments the structure of hadronic aggregates, the most familiar of which is the proton, following the principle of electron microscopy. In terms of figure 1b, the contribution of one of the particles to the overall structure of the interaction is nil. The most experimentally accessible particles which appear point–like relative to hadronic dimension are electrons (e^-) and positrons (e^+). The highest energy collisions between electrons (or positrons) and protons are to date those at HERA, in DESY, Hamburg, where 27.5 GeV electrons (or positrons) collide head–on with up to 920 GeV protons. HERA is the world's first collider of different species of particle. As such it is the electron microscope par excellence.

When they scatter at HERA, the electron and the proton interact extremely violently. The 4–momentum transfer squared Q^2 experienced by the electron is such that it resolves spatial distances of around 0.007 fm ($\Delta\boldsymbol{r} \sim \hbar/Q$ when $Q^2 \sim$ say 900 GeV² – equation 1). This is about 0.7 % of the diameter of the proton. The time scale of the interaction is at least a factor 10 shorter

1) By "peripheral" we mean the diffraction-like dependence in figure 2a which favours "glancing" interactions in which the protons change their directions only slightly

2) The values of Planck's constant in appropriate units are $\hbar c = 0.197$ GeV fm, and $\hbar = 6.58 \cdot 10^{-10}$ GeV fs.

than that characteristic of the constituent structure making up the proton ($\Delta T \sim \hbar/M_p c^2$ – equation 1). The scattering angular distribution of the electron thus reflects a "snapshot" (ΔT very small) of the finest detail ($\Delta \boldsymbol{r}$ very small) of proton structure.

The violence of such electron-proton collisions means that the target fragments; we say that the interaction $ep \to eX$ is deeply inelastic. Figure 3 shows one such electron–proton interaction in the H1 experiment at HERA. The incident electron scatters through substantial angle away from its incident (beam) direction and the proton fragments "opposite" to the electron because momentum has to be conserved in the interaction. Thereby the electron resolves one of the short distance constituents which make up the proton, a quark, and the quark appears as a "jet" of hadrons.

The inelastic nature of the interactions means that energy as well as momentum is transferred between the electron and the proton so that two variables describe the electron–proton interaction. They are most conveniently chosen to be 4–momentum transfer squared Q^2 and "Bjorken–x". When the electron-proton interaction is viewed in a Lorentz frame of reference in which the proton momentum exceeds greatly the electron momentum, x can be thought of as the fraction of the proton momentum carried by the quark which interacts with the electron (figure 4a).

The dependence on x and Q^2 of a "structure function" $F_2(x,Q^2)$ of the proton can be extracted from analysis of these interactions. The structure function specifies how the point–like constituents of the proton, the quarks, are distributed in x and Q^2 as seen by the electron which resolves and then interacts with one of them. The interaction between the point–like electron and the proton is envisaged as in figure 4a. If the charge of each "flavour", that is type, $u, d, \ldots$ of quark is e_i then

$$F_2(x,Q^2) = \sum_{i=u,d,\ldots} e_i^2 x f_i(x,Q^2)\,, \tag{2}$$

where $x f_i(x,Q^2)$ are "parton distribution functions" (pdf's) or parton densities specifying the distribution of the proton momentum amongst the quarks which make up the proton. If we understand the pdf's, we understand proton structure.

Measurements of F_2 now cover a large range of x and Q^2 (figures 5 and 6) [10, 11, 12, 13]. An unmistakable trend is observed. At lower x ($\lesssim 0.1$) F_2 rises with increasing Q^2, and more so as x decreases. At $x \sim 0.1$ F_2 is independent of Q^2. For $x \gtrsim 0.1$ F_2 decreases with increasing Q^2.

The lack of dependence at $x \sim 0.1$ of F_2 on Q^2 amounts to "scale invariance"; there is no dependence of the electron–proton scattering process on a distance scale (equation 1). The first measurements of F_2 in 1969 were mainly at such x [13]. When discovered, this

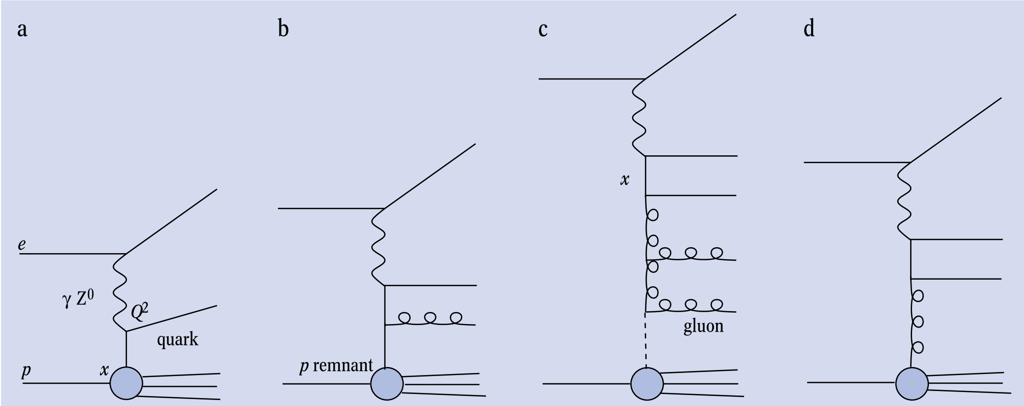

Fig. 4:
Schematic diagrams of an electron-proton (*ep*) interaction in which the electron interacts with the (spatially extended) proton. The process takes place in leading order by means of the exchange of a vector boson, either a photon γ or a Z^0, one of the massive electroweak bosons. The "blobs" in the diagrams correspond to the a priori unknown structure of the proton which, if the 4–momentum transfer squared Q^2 is large enough, can be resolved in the interaction. There is no unknown structure in the interaction other than that of the proton. The electron resolves the quark structure of the proton in that the exchanged vector boson couples to a quark in the proton.

▶ a) The electron resolves a quark in the proton structure.
▶ b) The electron resolves a quark in the proton after the quark has radiated a gluon and therefore carries less of the incident proton momentum.
▶ c) The electron resolves a quark in the proton which derives from a gluon which itself is part of a long "ladder" of gluon emissions; the resolved quark therefore carries much less of the incident proton momentum.
▶ d) The electron resolves a quark in the proton arising from the pair creation of quark and antiquark by a gluon associated with proton structure, boson–gluon fusion.

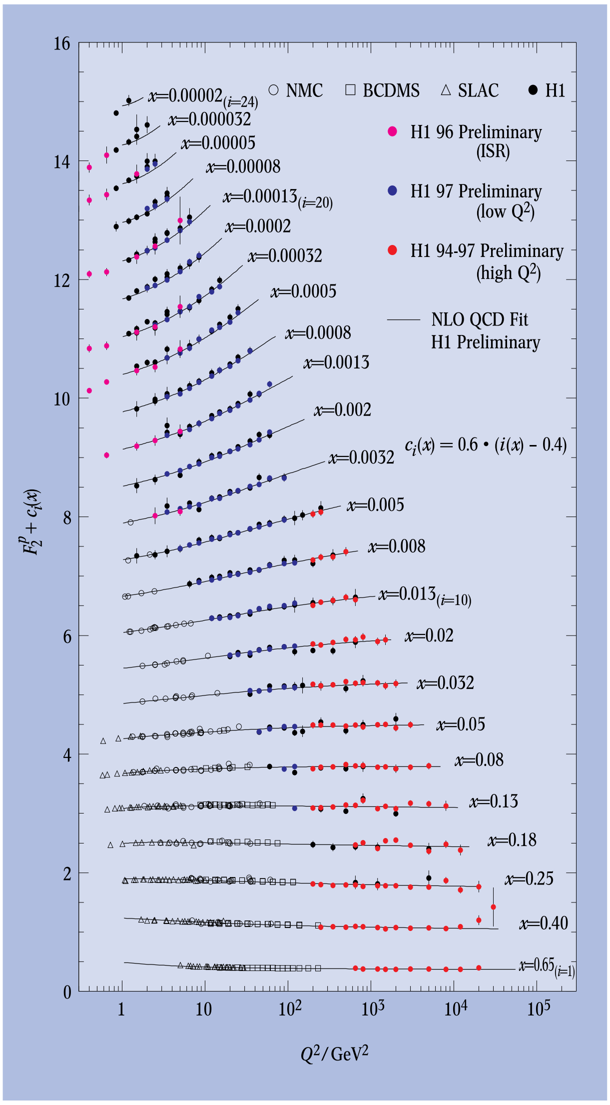

Fig. 5:
Measurements of the dependence of the proton structure function F_2 on Bjorken–x and Q^2; the results are displayed as dependences on Q^2 for different values of x; shown are H1 measurements [10] and lower energy measurements (NMC [11], BCDMS [12], SLAC [13]) in which stationary hydrogen targets were used together with high energy muon beams; a clear trend can be seen in the data: for larger Bjorken–x F_2 decreases with increasing Q^2 and for smaller Bjorken–x F_2 increases with increasing Q^2; the superimposed curves result from a fit assuming that proton structure is due to *uud* valence quarks interacting according to the expectations of QCD [16].

Fig. 6:
The measurements in figure 5 now in the form of a "reduced cross section", which is approximately F_2, for deeply inelastic electron–proton interactions at larger x only, showing more clearly the decrease with increasing resolution scale Q^2 for $x > 0.1$; there is also a discrepancy of low significance at the largest Q^2 at Bjorken–x of 0.45 where the data turn up and expectation, based on our total knowledge to date of proton structure and electron–quark interactions, says that the data should turn down.

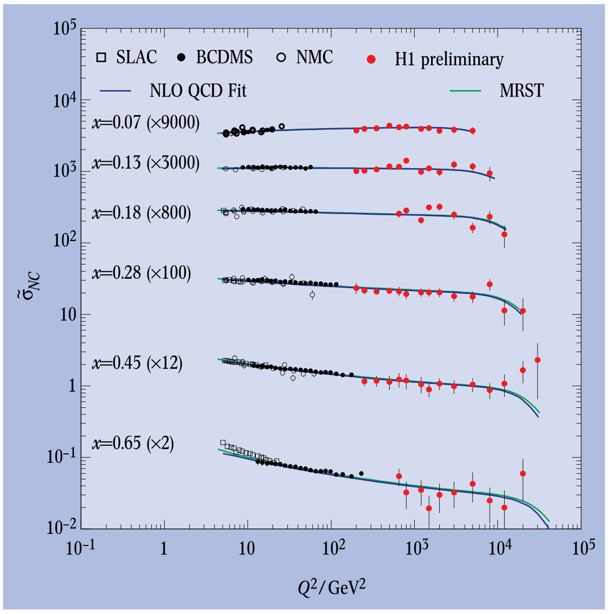

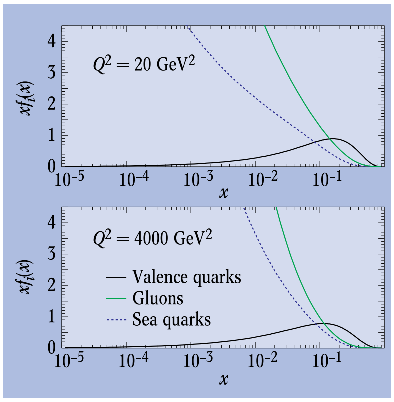

Fig. 8:
The proton as we now understand it from QCD fits to F_2 measurements; the parton distribution functions $x f_i(x)$ i = valence (uud), sea, and gluon of the proton are shown at two different "scales", or resolutions, $Q^2 = 20$ and 4000 GeV^2; the distributions show how, with increasing Q^2, the sea and gluon components grow and dominate at low x, and how the valence contribution evolves slowly to lower x.

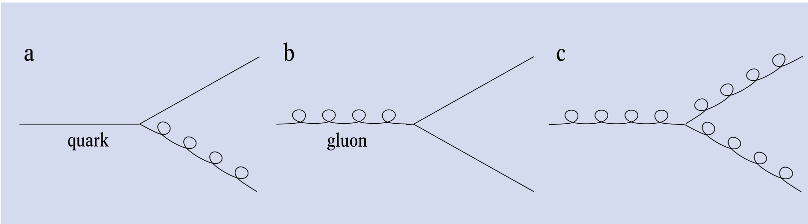

Fig. 7:
Feynman "vertices", or "splitting diagrams", in Quantum Chromodynamics (QCD) governing the interactions, and therefore also the quantum fluctuations, of the field quanta, quarks and gluons:
▶ a) gluon Bremsstrahlung by a quark $q \to qg$,
▶ b) gluon pair creation of a quark–antiquark pair $g \to q\bar{q}$,
▶ c) gluon pair creation of a gluon pair $g \to gg$. Gluons g appear as "springs", quarks q as lines.

scale invariance of deeply inelastic electron–proton scattering confirmed a prediction of Bjorken [14] and was the first evidence that the incident electron resolved and interacted with point–like (with no scale!), almost free, "partons" in the proton [15]. These partons were later identified as quarks (figure 4a).

Clearly, F_2 is not universally scale invariant – there is an "evolution" of quarks from larger to smaller fractional momentum x with increasing resolving power. With increasing Q^2 it becomes more and more likely that the electron interacts with a quark which carries less and less of the proton's momentum. Such violations of scale invariance (often colloquially referred to as "scaling violations") carry with them a simple message.

Because they are confined to form a proton, the quarks in a proton cannot be completely free; they must interact to some extent with each other. Any description of these interactions based on quantum field theory requires field quanta – gluons g – as well as quarks (just like the field quanta in quantum electrodynamics QED are photons as well as electrons). This quantum field theory is called quantum chromodynamics, or QCD, because in it the coupling strength is specified by a quantum number "colour" assigned to quarks and to gluons.

As in any quantum field theory, quantum fluctuations in QCD of the form of gluon Bremsstrahlung from quarks $q \to qg$ are possible (figure 7a) – compare QED Bremsstrahlung of photons. The interaction of the electron with a quark in the proton may therefore be after the quark has emitted one or more gluons when it then carries less of the proton's momentum (figures 4b and c). As the electron is able to resolve finer and finer detail in the proton, and thus finer and finer detail close to the quark, it is able to see the quark after it has lost momentum due to more and more gluon emissions. In this way a point–like quark looks different at different resolution scales – it has structure due to its quantum fluctuations. So as Q^2 increases the fraction of momentum x carried by the quarks is seen to evolve to lower values and more and more of the momentum of the proton becomes attributable to gluons. A feature of QCD is that the interaction between quarks becomes weaker as the distance between them gets smaller – "asymptotic freedom". Thus, when confined within a proton, quarks appear almost free and the structure of the proton can be expressed in such terms – equation 2 above.

There are also quantum fluctuations in QCD of the form of gluon pair production of quark and antiquark $g \to q\bar{q}$ (figure 7b) – compare e^+e^- pair production in QED – and also of two gluons $g \to gg$ (figure 7c) – for which there is no QED analogue. As Q^2 increases more and more quarks and antiquarks arising from gluon quantum fluctuations are also resolved by the electron. In this way the proton appears to the electron as having a density at low x of so called "sea" quarks and antiquarks which grows with increasing resolution and which is associated with the growing density of gluons. Thus as x decreases the rising dependence of F_2 on Q^2 becomes steeper.

The picture of proton structure outlined above can be quantified. The processes in figure 7 are calculable in QCD [16]. Parton distribution functions, or densities, $x f_i(x)$ can be extracted from the x and Q^2 dependence of F_2 (figure 5 and equation 2). Figure 8 shows the structure of the proton which is obtained at a low and at a high resolution scale Q^2 in terms of valence quark, sea quark and gluon pdf's $x f_{\mathrm{valence}}(x)$, $x f_{\mathrm{sea}}(x)$, and $x f_{\mathrm{gluon}}(x)$. With increasing resolution scale Q^2 the valence quark structure evolves slowly to lower x, and, at low x, the gluon and sea quark momentum densities grow.

So we have an understanding of proton structure based on the QCD dynamics of three valence quarks (uud) together inevitably with sea–quark and gluon densities which arise through quantum fluctuation. These features are epitomised in the nature of the scaling violations at different x. At low x, where gluon pair production is important, the structure function F_2 of the proton rises with increasing Q^2 (figure 5), and at larger x, where gluon Bremsstrahlung from valence quarks is important, F_2 falls with increasing Q^2 (figure 6). The original scale invariance first observed at $x \sim 0.1$ arises from a balance of two contrasting consequences of quantum fluctuations in QCD together with the distribution functions specifying the quark and gluon densities in the proton.

The Structure of the Photon

Unlike the proton, the photon is a field quantum with well prescribed "point–like couplings" to other electrically charged field quanta, such as electrons, positrons and quarks. The existence of quantum fluctuations of the photon to these charged quanta means that a photon will thereby also have a "structure", the detail of which is visible to the extent that it can be resolved by a probe.

Quantum fluctuations of a photon to electrons and positrons contribute to the QED structure of the photon. The most notable consequence of such structure is the anomalous magnetic moment (g–factor >2) of the electron. The effect of quantum fluctuation is also manifest in atomic spectroscopy – the Lamb shift [17]. Another consequence is electron–positron pair production $\gamma \to e^+e^-$ by high energy (for example X– and γ–ray) photons.

There are also quantum fluctuations of the photon to quark and antiquark $\gamma \to q\bar{q}$, and thus there is expected to be a QCD, or hadronic, structure of the photon. Observation of this structure is therefore a test of our QCD–based picture of hadronic physics. Moreover, just as for the QED structure of the photon, Witten showed that the QCD structure could be calculated [18].

In analogy with deeply inelastic electron-proton interactions and proton structure, hadronic photon structure can be observed in deeply inelastic electron-photon interactions (figure 9) in the process $e^+e^- \to e^+e^-X$ (X is a hadronic system). One electron[3)] scatters with a momentum transfer squared Q^2 and the other with P^2. It is possible to arrange P^2 to be less than Q^2 in which case one electron interacts more violently with momentum transfer squared Q^2 and so probes the hadronic structure of the "target" photon of mass squared P^2 arising from a less violent electron interaction. The kinematic variables Q^2 and x have the same definition and physical meaning as for deeply inelastic electron–proton scattering, and we can measure structure functions of photons of different mass squared P^2.

3) Here no distinction is made between electron and positron because it is not necessary – the term electron is generic.

The first measurements of the photon structure function F_2^γ were made at the PETRA e^+e^- storage rings at DESY in the early 1980s. An example is shown in figure 10a [19] for the easiest case to measure, namely when P^2 is very nearly zero so that the "target" photon is very nearly real. The x–dependence of F_2^γ shows a tendency to increase, and there are clear scaling violations in which F_2^γ everywhere rises with increasing Q^2.

The Q^2 dependence of F_2^γ follows that expected if hadronic photon structure is dominated by quantum fluctuation. Quark antiquark splitting $\gamma \to q\bar{q}$ is very like gluon splitting $g \to q\bar{q}$. At low–x where gluon splitting dominates proton structure, the scaling violations of F_2

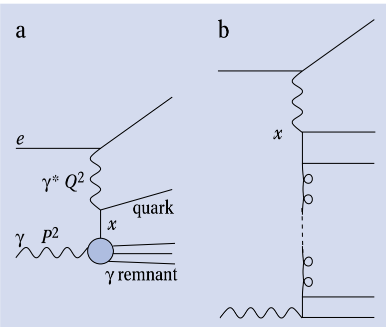

Fig. 9:
Schematic diagrams of an electron–photon ($e\gamma$) interaction in which the electron interacts with the QCD driven structure of the photon. The electron resolves the quark structure of the photon in that the exchanged vector boson couples to a quark in the photon.
▶ a) The electron resolves a quark in the photon structure;
▶ b) the electron resolves a quark in the photon after the quark has radiated a gluon which itself then radiates more gluons before producing the resolved quark, which now therefore carries much less of the incident proton momentum.

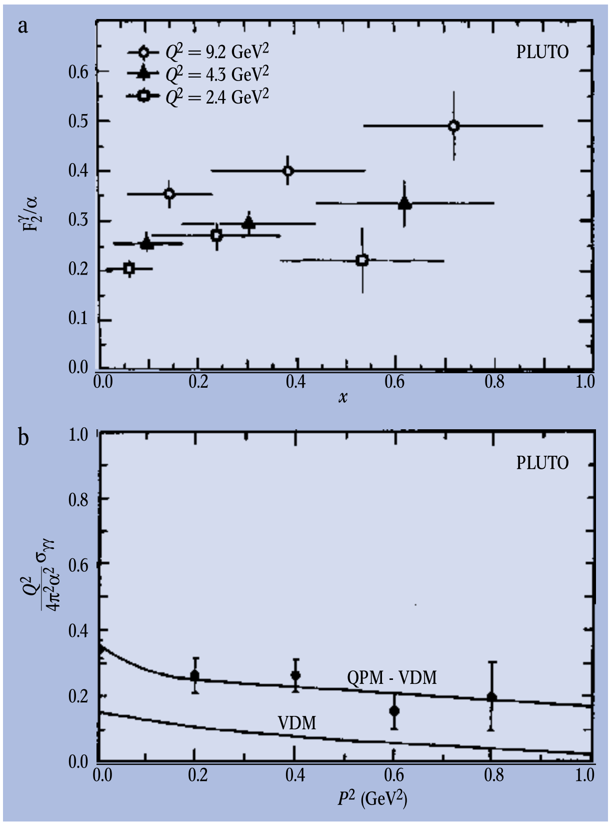

Fig. 10:
▶ a) An early measurement of the photon structure function F_2^γ in deeply inelastic $e\gamma$ data using $e^+e^- \to e^+e^-X$ interactions; the x dependences are shown as a function of Q^2, where scaling violations are visible in which F_2^γ increases with increasing Q^2 for all x, at a fixed Q^2 the x–dependence of F_2^γ shows a tendency to rise with increasing x, as expected if the structure is driven by the quantum fluctuation $\gamma \to q\bar{q}$ in QCD. HAD specifies the contribution estimated from the fluctuation of the photon into a resonance; QPM(c) is an estimate of the charm quark contribution.
▶ b) A measurement of the dependence on the target photon mass squared P^2 of the virtual photon (γ^*) structure function F_2^γ at fixed probe scale Q^2 in deeply inelastic $e\gamma^*$ interactions using $e^+e^- \to e^+e^-X$ data; the curves are the expectations based on QCD. QPM refers to the contribution from the quantum fluctuation $\gamma^* \to q\bar{q}$ and VDM to an estimate of additional contributions

rise with increasing Q^2 (section 3 and figure 5). So the rising scaling violations of F_2^γ over the whole range of x which is measured follow the expectation of a structure driven by the quantum fluctuation $\gamma \rightarrow q\bar{q}$. Moreover, an understanding of such measurements of F_2^γ in terms of ab initio calculations of hadronic photon structure in QCD (following Witten) has been achieved.

We can also test further the QCD picture of photon structure by increasing the mass squared P^2 of the "target" photon, that is by "squeezing it" ($\Delta \mathbf{p} \sim P$ larger, so $\Delta \mathbf{r}$ smaller – equation 1). The parent electron of the target photon is thus required to scatter through somewhat larger scattering angles thereby increasing P^2. The only such measurement until recently was also made at the PETRA e^+e^- storage rings [20] in the early 1980s. The results demonstrate that, as the size of the photon decreases, its hadronic structure diminishes broadly as expected in QCD (figure 10b).

Nowadays new measurements of real and virtual photon structure are available from experiments at e^+e^- colliders such as LEP [21] and, using a different experimental approach, from experiments at HERA [22, 23].

So the hadronic structure of the photon is the archetype for the structure of point-like quanta through quantum fluctuation. It is driven by a leading splitting function $\gamma \rightarrow q\bar{q}$ in which the scaling violations of the structure function show a rise with increasing Q^2 for all but the largest x, and for which the x dependence of the structure function tends to increase with increasing x. Furthermore, ab initio QCD calculations of photon structure are found to be broadly consistent with measurement.

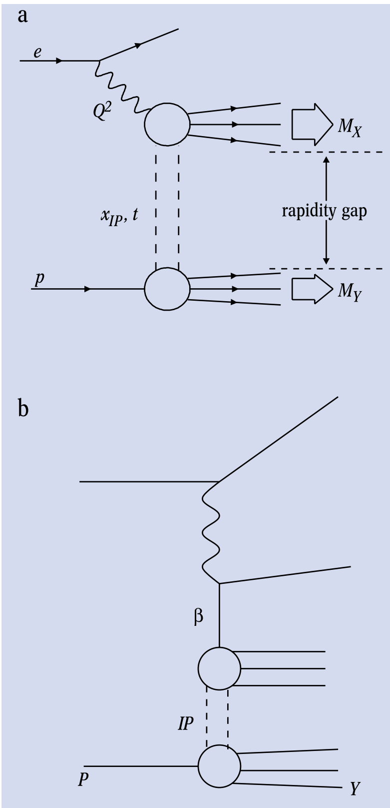

Fig. 11:
Schematic "Feynman diagrams" of a deep-inelastic *ep* interaction at low Bjorken-*x* in which there is a rapidity gap between the proton remnant *Y* and other produced hadrons *X*.
▶ a) The presence of the rapidity gap allows two hadronic system *X* and *Y* to be distinguished. The mass of system *Y* is constrained to be less than 1.6 GeV by means of forward secondary particle detectors. The mass M_X of system *X* is measured in the central region of the experiment.
▶ b) If such interactions are viewed as deeply inelastic scattering then they amount to a probe of the structure of the momentum transfer in the proton interaction $p \rightarrow Y$ in which the quark resolved by the electron is part of the structure of the interaction rather than the structure of the proton; β is the Bjorken-x momentum variable for the resolved quark now as a fraction of the momentum transfer $\mathbb{P} = P - Y$ in the interaction.

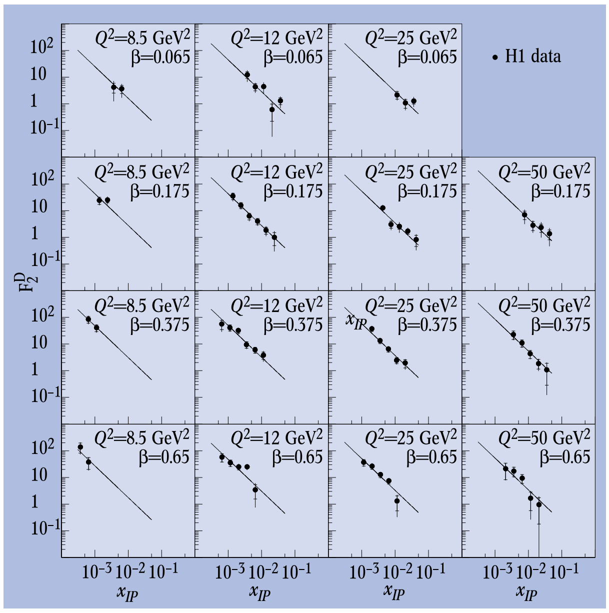

Fig. 12:
The first measurement of the structure function $F_2^{D(3)}(\beta, Q^2, x_\mathbb{P})$ [26]; the $x_\mathbb{P}$ dependence is shown for different fixed values of Q^2, the deep-inelastic probe scale, and β; the curves are the result of a fit in which a universal diffractive dependence, corresponding closely to that in inelastic *pp* interactions, is fitted to the data.

The Structure of Hadronic Interactions

Proton structure at low x is dominated by the consequences of QCD quantum fluctuations, namely by sea-quarks and gluons and their growth with increasing probe resolution Q^2 (figure 8). A long "chain", or "ladder", of QCD radiation in the form of gluon and quark emission can occur before the electron interacts with a quark – figure 4c, and the quark now has perforce only a tiny fraction x left of its parent proton's momentum.

A consequence of such a ladder is the way in which hadrons are distributed in the final state of the deeply inelastic electron-proton interaction. As we have seen (figure 3), quarks appear as single identifiable "jets" of hadrons. The presence of a ladder of emissions means therefore that hadrons from this QCD radiation must appear between the direction of the quark which is resolved by the electron "at the top of the ladder" and the remnant of the proton "at the bottom of the ladder".

In an interaction in which the electron resolves the quark after substantial QCD radiation, as in figure 4c, it is of course something of a matter of choice as to whether one still considers the quark as part of the structure of the proton, or more as a consequence of the interaction with which we observe it. Thus one may begin to see how the ladders which can occur in deeply inelastic scattering can better be thought of as part of the structure of the electron-proton interaction, rather than as part of the structure of the proton.

There are however also deeply inelastic electron-proton interactions in which there is no hadron production adjacent to the proton beam direction – so called "rapidity gap" interactions – and they correspond topologically to figure 11a [24, 25]. Two hadronic systems, X and Y, are distinguished between which there is no other hadron production. System Y remains undetected continuing in a direction close to that of the incident proton. Thus the incident proton's interaction $p \to Y$ is peripheral (as in a high energy interaction with another hadron – section 2). The electron, on the other hand, has substantial resolving power Q^2. As figures 11a and b imply, the interactions $ep \to eXY$ are thereby concerned more with the structure of the peripheral proton interaction, and less with the structure of the proton itself. In the old phenomenological picture in which we understand hadronic interactions in terms of the exchange of hadrons (Yukawa and Regge – section 2), we probe the structure of the exchanged system of hadrons, whatever that may be.

> *"A future theory must be unitary in a very wide sense; it must connect all the present theories of particles and their interactions in a single rational system."*
> *Max Born [1]*

Interactions of the form $ep \to eXY$ in figure 11 can be described with the variables Q^2 and x, and the additional variables 4–momentum transfer squared t and $x_{\mathbb{P}}$ (section 2). Here $\mathbb{P}$ is the 4–momentum vector specifying the transfer in the proton interaction $p \to Y$, i. e. $\mathbb{P} = P - Y$ and $t = \mathbb{P}^2$. In the picture pioneered by Yukawa and Regge (section 2), the 4–momentum transfer vector $\mathbb{P}$ corresponds to that of the exchanged particle(s), and $x_{\mathbb{P}}$ is this momentum as a fraction of the incident proton momentum P (see also figure 2).

The variable $\beta = x/x_{\mathbb{P}}$ is also introduced to specify the fraction of the momentum $\mathbb{P}$ which is taken by the quark in its interaction with the electron (figure 11b). Thus β plays the role of a fractional momentum variable for the deeply inelastic scattering of the electron by the momentum transfer $\mathbb{P}$ (like x for the deeply inelastic scattering of the electron by the proton).

The dependence of a structure function $F_2^{D(3)}$ on β, $x_{\mathbb{P}}$ and Q^2 can be extracted. At fixed $x_{\mathbb{P}}$, $F_2^{D(3)}$ specifies the deeply inelastic structure of the energy/momentum transfer $\mathbb{P}$ in the proton interaction (figure 11b) in an analogous way to that in which the structure functions F_2 specifies the deeply inelastic structure of the proton.

Figure 12 shows the first measurement [26] of the $x_{\mathbb{P}}$ dependence of $F_2^{D(3)}(\beta, Q^2, x_{\mathbb{P}})$ for different values of Q^2 and β. Clearly this structure function falls sharply with increasing $x_{\mathbb{P}}$ in an approximately universal manner, very much like the cross section for high energy inelastic proton–proton interactions ($pp \to XY$ – figure 2 and section 2). Thus the inelastic proton interaction $p \to Y$ in $ep \to eXY$ is very much like its interaction in an inelastic diffractive interaction $pp \to XY$.

To try to understand the structure of the proton interaction we resort as before to the dependence on resolution scale Q^2 of the structure function $F_2^{D(3)}$. Figure 13 shows the Q^2 dependences at fixed $x_{\mathbb{P}}$ for different β [27, 28]. There are again "scaling violations" which show a slow rise with increasing Q^2 at all but the largest β. As for both proton structure at low x (figure 5) and photon structure (figure 10a), they signal that the structure of the proton interaction is driven in large part by gluon quantum fluctuation. This is presumably because the momentum transfer $\mathbb{P}$ is associated with a gluon–dominated hadronic structure which is only resolved by the probing electron after the quantum fluctuation $g \to q\bar{q}$. Furthermore the β dependence of $F_2^{D(3)}$ (not shown directly but apparent in figure 12) is relatively featureless, reminiscent of that of the photon structure function (figure 10a).

Unlike the case of the photon and like the case of the proton, successful ab initio calculation in QCD remains elusive because the QCD structure of $\mathbb{P}$ must involve more than one gluon. However, application of the same theoretical "QCD machinery" which is used to fit the proton structure function F_2 (section 3) confirms the conclusion of gluon dominance of $\mathbb{P}$ and thus the structure of the proton interaction (figure 13) [27].

These measurements at HERA of the deeply inelastic structure of hadronic interactions have challenged QCD theory. The interpretation in terms of gluon dominance, which is based on the persistence of rising scaling violations for all but the largest values of the fractional momentum variable β, is now confirmed in other measurements [29, 30, 31, 32].

Into the Future

It is of course of paramount importance to strive to extend the precision of the probe which we have to look at the deepest structure of hadrons and their interactions. Already HERA has revealed hints of its uniquely important future in such physics – figure 6 [10].

At the highest Q^2 the status of measurements of the scale dependence of positron–proton scattering is tantalising because of the present experimental limits in accuracy. Overall there is no evidence for any breakdown of our present understanding of proton structure, in that the curves in figure 6 do not deviate significantly from the measurements throughout the whole range of resolution scale Q^2. However notice that there is a suggestion of a discrepancy at the highest $Q^2 \sim 10^4$ GeV^2 and at $x = 0.45$ where the experimental uncertainty is greatest and where the results suggest a "turn up" [33, 10]. Expectation says that the results should here "turn down". Only with more data, which will come soon at HERA, can such a discrepancy be established, or otherwise, and possible new electron-quark physics established.

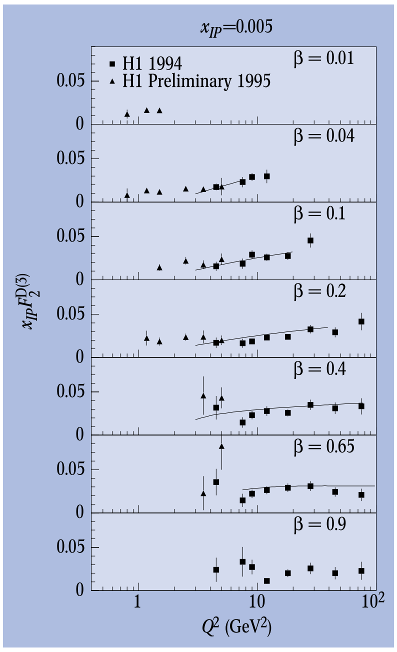

Fig. 13:
The Q^2 dependences of $x_{\mathbb{P}}F_2^{D(3)}(\beta, Q^2, x_{\mathbb{P}})$ at $x_{\mathbb{P}} = 0.005$ for different β [27,28]; superimposed is a fit to the results in which it is found that the structure of the proton interaction has contributions from predominantly gluons at a starting scale of $Q^2 = 3$ GeV^2; at $Q^2 = 3$ GeV^2 roughly 90 % of the momentum transfer in the proton interaction is found to be carried by gluons.

Conclusion

Understanding the structure of hadronic physics is a pre–requisite in our quest for the ultimate laws of nature. It is today's frontier in the noble pursuit of the structure of matter which has so dominated 20th century physics. After decades of experimentation, guided by the simplest principle of Quantum Mechanics, we have a theory of hadronic physics, Quantum Chromodynamics or QCD.

However, ab initio prediction with this theory continues to pose many challenges. Calculations from first principles of either the structure of a hadron or the way hadrons interact prove to be extremely challenging. Progress to date continues to involve a close symbiosis of experiment and theory to understand the dependences on resolution scale when probing different hadronic phenomena. The future will be no exception – new physics will be manifest in the form of evidence for new hadronic structure. The HERA electron microscope is the most precise and comprehensive tool which we have in this quest.

Epilog

Ich empfinde es als großes Privileg und Ehre, die Max Born Medaille und den Preis 1999 des Institute of Physics und der Deutschen Physikalischen Gesellschaft verliehen zu bekommen. Ich danke beiden für diese Anerkennung meines Wirkens. Eine vernünftige Betrachtungsweise der Arbeit und des Lebens eines Experimentalphysikers in der Hochenergiephysik kann jedoch nur diejenige sein, die ihn als kleinen Teil einer immensen Teamarbeit darstellt. In der Zusammenarbeit mit all denen, deren Fähigkeiten sich so großartig ergänzen, wird das ganze Unterfangen angetrieben vom gemeinsamen Glauben an die Faszination, den Wert und die Bedeutung des Wunsches der Menschheit, seine Welt zu verstehen. Für mich steht deshalb außer Zweifel, daß die Verleihung dieses Preises vor allem die großen Fähigkeiten der beteiligten Kollegen widerspiegelt. Darunter sind viele Mitarbeiter aus verschiedenen Instituten und von verschiedenen Experimenten. Ich danke ihnen für die Geduld und vor allem die vielen anregenden Phasen, die wir zusammen erleben konnten.

Natürlich spielt DESY unter all diesen Instituten eine besondere Rolle. Ich hatte das Glück, über mehr als zwanzig Jahre an dem großartigen, wissenschaftlichen Abenteuers teilzunehmen, das die Grundlage der Existenz dieses Labors bildet. Ich nutze deshalb den heutigen Anlaß, meinen Respekt und meinen Dank all denen auszusprechen, die DESY weiterhin zu dem machen, was es heute darstellt, angefangen beim Steuerzahler bis hin zum Direktor.

Ich kann diesen Vortrag nicht beenden, ohne den erst kurz zurückliegenden tragischen und völlig unerwarteten Tod des DESY Direktors Professor Björn Wiik zu erwähnen. Sein plötzliches Fehlen am DESY wird für Jahre zu spüren sein. Sein positiver, unterstützender und unaufdringlicher Einfluß war stets präsent in unserem Wirken. Seine Sicht der Zukunft von DESY und damit der Zukunft der Hochenergiephysik bleibt uns. Es ist eine anregende Vision und das Erreichen des Ziels wird mit Recht ein bleibendes Zeichen seiner Erinnerung darstellen.

References

[1] *M Born*, “Atomic Physics”, Blackie and Son Limited, Seventh Edition 1962, reprinted 1965, translated from “Moderne Physik” and revised with *R J Blin-Stoyle*

[2] *W Heisenberg*, Z. Phys. **43** (1927) 172

[3] *M Born, W Heisenberg, P Jordan*, Z. Phys. **35** (1925) 557

[4] *R M Barnett et al.*, Phys. Rev. **D54** (1996) 1 and 1997 off-year partial update for the 1998 edition available on the PDG WWW pages (URL: http://pdg.lbl.gov/), and references therein.

[5] *M Gell–Mann*, Phys. Lett. **8** (1964) 214; *G Zweig*, CERN Report 8419/Th (1964) 412

[6] *A Breakstone et al.*, Phys. Rev. Lett. **54** (1985) 2180

[7] *R Cool et al.*, Phys. Rev. Lett. **47** (1981) 701

[8] *H Yukawa*, Proc. Phys. Math. Soc. Japan **17** (1935) 48

[9] *T. Regge*, Nuov. Cim. **14** (1959) 951, Nuov. Cim. **18** (1960) 947; *G. Chew, S. Frautschi, S. Mandelstam*, Phys. Rev. **126** (1962) 1202

[10] *H1 Collaboration*, “Measurement of Inclusive Cross Sections for Neutral and Charged Current Interactions at High-Q^2”, paper 533; *H1 Collaboration*, “Precision Measurement of the Inclusive Deep Inelastic ep Scattering Cross Section at Low Q^2 at HERA”, paper 534; *H1 Collaboration*, “Low Q^2 – Intermediate x Structure Function Measurement at HERA”, paper 535; papers submitted to the 29th International Conference on High-Energy Physics, 22-30 Jul 1998, Vancouver, Canada; *H1 Collaboration, S Aid et al.*, Nucl. Phys. **B497** (1997) 3, *H1 Collaboration, S Aid et al.*, Nucl. Phys. **B470** (1996) 3

[11] *NMC Collaboration, M Arneodo et al.*, Nucl. Phys. **B483** (1997) 3

[12] *BCDMS Collaboration, A C Benvenuti et al.*, Phys. Lett. **B223** (1989) 485

[13] *E D Bloom et al.*, Phys. Rev. Lett. **23** (1969) 930; *M Breidenbach et al.*, Phys. Rev. Lett. **23** (1969) 93

[14] *J D Bjorken*, Phys. Rev. **163** (1967) 1767; *Phys. Rev.* **179** (1969) 1547

[15] *R P Feynman*, Phys. Rev. Lett. **23** (1969) 1415

[16] *Yu L Dokshitzer*, JETP **46** (1977) 641; *V N Gribov and L N Lipatov*, Sov. Journ. Nucl. Phys. **15** (1972) 78; *G Altarelli and G Parisi*, Nucl. Phys. **B126** (1977) 298

[17] *W E Lamb and R C Retherford*, Phys. Rev. **72** (1947) 241

[18] *E Witten*, Nucl. Phys. **B120** (1977) 189

[19] *PLUTO Collaboration, Ch Berger et al.*, Phys. Lett. **142B** 111

[20] *PLUTO Collaboration, Ch Berger et al.*, Phys. Lett. **142B** 119

[21] *OPAL Collaboration, K Ackerstaff et al.*, Phys. Lett. **B412** (1997) 225; *OPAL Collaboration, K Ackerstaff et al.*, Phys. Lett. **B411** (1997) 387; *OPAL Collaboration, K Ackerstaff et al.*, Z. Phys. **C74** (1997) 33

[22] *H1 Collaboration, C Adloff et al.*, Eur. Phys. J. **C1** (1998) 97

[23] *H1 Collaboration, C Adloff et al.*, “Measurement of Dijet Cross-Sections at Low Q2 and the Extraction of an Effective Parton Density for the Virtual Photon”, DESY-98-205, to appear in Eur. Phys. J. **C**

[24] *ZEUS Collaboration, M Derrick et al*, Phys. Lett. **B315** (1993) 481

[25] *H1 Collaboration, T Ahmed et al.*, Nucl. Phys. **B429** (1994) 477

[26] *H1 Collaboration, C Adloff et al.*, Phys. Lett.**B 348** (1995) 681

[27] *H1 Collaboration, C Adloff et al.*, Zeit. Phys. **C76** (1997) 613

[28] *H1 Collaboration*, “Measurement and Interpretation of the Diffractive Structure Function $F_2^{D(3)}$ at HERA”, paper 571 submitted to the 29th International Conference on High-Energy Physics, 22-30 Jul 1998, Vancouver, Canada

[29] *H1 Collaboration, C Adloff et al.*, Phys. Lett. **B428** (1998) 206

[30] *H1 Collaboration, C Adloff et al.*, Eur. Phys. J. **C1** (1998) 495

[31] *H1 Collaboration, C Adloff et al.*, Eur. Phys. J. **C6** (1999) 421

[32] *H1 Collaboration, C Adloff et al.*, Eur. Phys. J. **C5** (1998) 439

[33] *H1 Collaboration, C Adloff et al.*, Z. Phys. **C74** (1997) 191